16th IEEE International Conference on Control Applications
Part of IEEE Multi-conference on Systems and Control
Singapore, 1-3 October 2007

Control and Rotation Rate Estimation of Vibrational MEMS Gyroscopes[1]

Qing Zheng[2], *Student Member*, *IEEE*, Lili Dong[2, *], *Member*, *IEEE,* Zhiqiang Gao[2], *Member, IEEE*

***Abstract*— There are two major control problems associated with vibrational MEMS gyroscopes: to control two vibrating axes (or modes) of the gyroscope, and to estimate a time-varying rotation rate. This paper demonstrates how a novel active disturbance rejection control addresses these problems in the presence of the mismatch of natural frequencies between two axes, mechanical-thermal noises, Quadrature errors, and parameter variations. A demodulation approach based on the estimated dynamics of the system by an extended state observer is proposed to estimate the rotation rate. The simulation results on a Z-axis MEMS gyroscope show that the controller is very effective by driving the output of the drive axis to a desired trajectory, forcing the vibration of the sense axis to zero for a force-to-rebalance operation and precisely estimating the rotation rate.**

I. INTRODUCTION

MEMS gyroscopes are inertial rate sensors batch fabricated on crystal silicon or polysilicon [1]. A Z-axis MEMS gyroscope is sensitive to the rotation rate about the Z axis normal to the plane of silicon chip. A vibratory Z-axis MEMS gyroscope developed by Berkeley Sensor and Actuator Center [2] is shown in Fig. 1. The operating principle of MEMS gyroscopes is based on the energy transfer from driving mode to sensing mode of gyroscopes caused by Coriolis acceleration. When the gyroscope is subject to a rotation rate, the response of the sensing mode provides the information of the rotation rate. With the advancement of MEMS technology, MEMS gyroscopes have been applied to automobiles for roll-over sensors and skid control, consumer electronics (e.g. camera stabilizations), GPS assisted inertial navigation, industry, aerospace, and so on [3]. However, fabrication imperfections and environmental variations produce undesirable coupling terms, unknown disturbances, input and measurement noises, frequency mismatch between two vibrating modes, and parameter variations which degrade the performance of the gyroscopes. As a consequence, a control system is essential to improve the performance and stability of MEMS gyroscopes. Advanced control technologies should focus on exploiting the inherent structures of the vibratory MEMS gyroscopes, so as to achieve disturbance attenuation and performance robustness against modeling uncertainties.

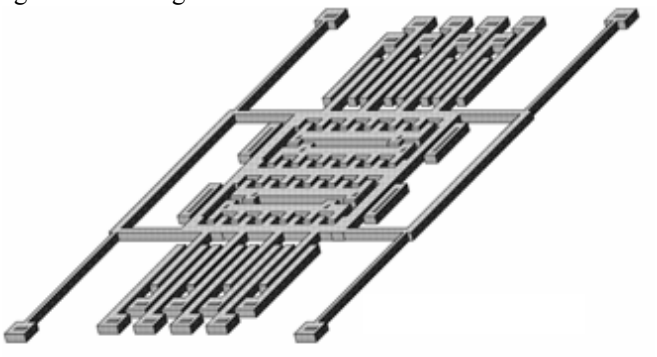

Fig.1. Photo of a vibratory Z-axis MEMS gyroscope [2].

Since the 1990's, there has been substantial research on the control designs of MEMS gyroscopes. Most of the reported control approaches [4-8] assume constant rotation rate. In reality, however, the rotation rate is time varying. The adaptive controllers reported in [9, 10] are designed to approximate a time-varying rotation rate, but the multiple tuning parameters of the controllers in [9, 10] make them difficult to implement in real world situation. Hence, dealing with such time-varying uncertain dynamics of MEMS gyroscopes makes the control problem challenging and critically important. Since the system dynamics are only partially known, a solution that is insensitive to the uncertainties in system dynamics and is able to accurately determine the rotation rate is needed.

In this paper, a new control solution known as active disturbance rejection control (ADRC) is introduced to MEMS gyroscopes. The ADRC was first proposed by Han [11-13] and further parameterized in [14] and explicated in [15]. ADRC as a practical design method has been successfully applied in many engineering applications, such as motion control [16-18], aircraft flight control [19], and voltage regulation in DC-DC power converter [20], etc. The basic idea of this control strategy is to use an extended state observer (ESO) to estimate the plant dynamics and unknown disturbances in real time and dynamically compensate for it. In this paper, ADRC is used to control the MEMS gyroscope. In particular, the ESO provides an estimate of the combination of the external disturbances and plant dynamics, which has modeling errors and structure uncertainties due to the unknown time varying rotation rate and the unknown Quadrature error terms arising from mechanical imperfections. In addition, with the accurate

[1]The work is supported by Ohio ICE (Instrumental, Control, and Electronic) consortium under grant 0260-0652-10.

[2]The authors are with the Department of Electrical and Computer Engineering, Cleveland State University, Cleveland, OH 44115, USA.

[*]The corresponding author. Email: L.Dong34@csuohio.edu, Tel: 1-216-687-5312, Fax: 1-216-687-5405.

estimate of the plant dynamics, an input time-varying rotation rate is accurately estimated with the demodulation technique.

This paper is organized as follows. The dynamics of MEMS gyroscope is described in Section II. The ADRC approach is presented in Section III. The rotation rate estimation law is developed in Section IV. The simulation results are shown in Section V. Finally, some concluding remarks are given in Section VI.

II. DYNAMICS OF MEMS GYROSCOPES

The mechanical model of a Z-axis MEMS gyroscope is shown in Fig. 2. The gyroscope is only sensitive to the rotation rate about Z axis in the associated Cartesian reference frame. The Z-axis MEMS gyroscope can be simplified as a two-degree-of-freedom structure. The proof mass is suspended above the substrate by a set of polysilicon beams functioning like springs. All the forces against the movement of the proof mass contribute to damping forces. In Fig. 1, the rigid frame of the gyroscope is rotating about the rotation axis (Z axis) with a rotation rate of Ω while it is driven to resonance along the drive axis (X axis). Simultaneously a Coriolis acceleration, illustrated in Fig. 3, is produced along the sense axis (Y axis) which is perpendicular to both drive and rotation axes. As shown in Fig. 3, the Coriolis acceleration is proportional to both the applied rotation rate and the amplitude of the velocity of the moving mass along the drive axis. Therefore we can determine the rotation rate through sensing the vibration of the sense axis.

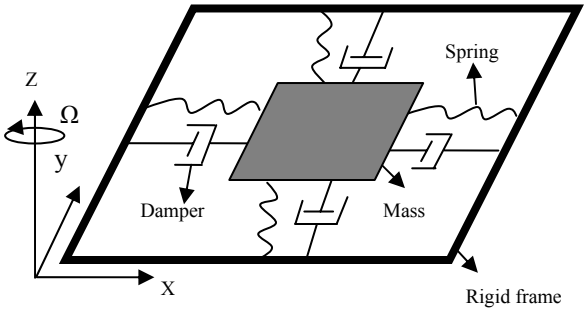

Fig. 2. A model of a Z-axis MEMS gyroscope.

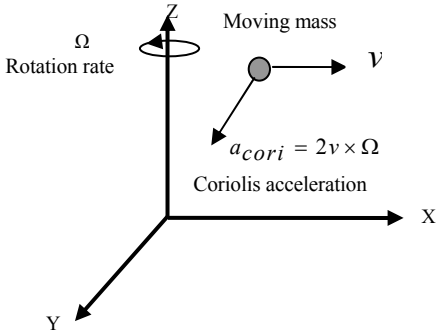

Fig. 3. The concept of Coriolis acceleration.

We assume there is no coupling in the damping for both the drive and sense axes. We allow for the frequency mismatch between the two axes. The governing equations of the Z-Axis MEMS gyroscope [5] are represented by

$$\begin{cases} \ddot{x} + 2\zeta\omega_n \dot{x} + \omega_n^2 x + \omega_{xy} y - 2\Omega\dot{y} = \dfrac{K}{m} u_d(t) \\ \ddot{y} + 2\zeta_y \omega_y \dot{y} + \omega_y^2 y + \omega_{xy} x + 2\Omega\dot{x} = \dfrac{K}{m} u_s(t) \end{cases} \tag{1}$$

where $x(t)$ and $y(t)$ are drive axis and sense axis outputs respectively, ω_n and ω_y are natural frequencies of drive and sense axes, ζ and ζ_y are damping coefficients, u_d and u_s are control inputs for the drive and sense axes, m is the proof mass, $2\Omega\dot{x}$ and $2\Omega\dot{y}$ are Coriolis accelerations, Ω is an unknown time-varying rotation rate, $\omega_{xy}y$ and $\omega_{xy}x$ are constant unknown Quadrature error terms caused by stiffness couplings between two axes, and K is a constant that accounts for sensor, actuator, and amplifier gains.

Rotation sensing is achieved by forcing the drive axis into a fixed amplitude vibration, and measuring the displacement y(t) of sense axis. We apply force-to-rebalance mode of operation onto the sense axis because of the general success of nulling-the-output approach in precise sensing applications [4]. In this mode, the output amplitude of the sense axis is continuously monitored and driven to zero, and the control signal becomes a part of measurement of rotation rate. Therefore our control tasks are to drive the drive axis to the desired trajectory with specified amplitude and resonant frequency, to force the output of the sense axis to zero, and to estimate the rotation rate in the presence of noises.

III. ACTIVE DISTURBANCE REJECTION CONTROL

Most existing control approaches for MEMS gyroscopes employ various methods to derive the accurate model of the plant. However, in practice, it is very challenging to achieve the precise model information. Especially for MEMS gyroscope, the factors such as the mechanical-thermal noise, the measurement noise, the unknown time varying rotation rate, and the unknown Quadrature error terms, bring modeling errors and structural uncertainties in the system. The mechanical imperfection and environmental variations also introduce the parameter variations to the model of MEMS gyroscopes. ADRC is a natural fit for the MEMS gyroscope control due to its inherent disturbance rejection characteristics. The idea of ADRC is briefly introduced as follows.

The MEMS gyroscope can be understood as a coupled second-order system. The system (1) can be rewritten as

$$\begin{cases} \ddot{x} = -\left(2\zeta\omega_n \dot{x} + \omega_n^2 x + \omega_{xy} y - 2\Omega\dot{y}\right) + b_x u_d \\ \ddot{y} = -\left(2\zeta_y \omega_y \dot{y} + \omega_y^2 y + \omega_{xy} x + 2\Omega\dot{x}\right) + b_y u_s \end{cases} \tag{2}$$

where $b_x = b_y = \dfrac{K}{m}$.

Define

$$\begin{cases} f_x = -\left(2\zeta\omega_n\dot{x} + \omega_n^2 x + \omega_{xy} y - 2\Omega\dot{y}\right) \\ f_y = -\left(2\zeta_y\omega_y\dot{y} + \omega_y^2 y + \omega_{xy} x + 2\Omega\dot{x}\right) \end{cases} \quad (3)$$

where f_x and f_y are referred to as the generalized disturbance, or disturbance, because they represent both the unknown internal dynamics and the external disturbances of the drive and sense axes respectively. The couplings between the two axes are also taken as disturbances to each axis. Substituting (3) into (2), the system (2) becomes

$$\begin{cases} \ddot{x} = f_x + b_x u_d & (4-1) \\ \ddot{y} = f_y + b_y u_s . & (4-2) \end{cases}$$

The basic idea of ADRC is to obtain the estimated f_x and f_y, i.e., $\hat{f}_x$ and $\hat{f}_y$, and to compensate for them in the control law in real time. Note that the control designs of the drive and sense axes are the same and they are implemented in parallel. For clarity, the concept of ADRC is explained with the control of the sense axis in the following.

Let $\xi_{y1} = y, \xi_{y2} = \dot{y}$, $\xi_{y3} = f_y$ and $\xi_y = [\xi_{y1}, \xi_{y2}, \xi_{y3}]^T$. Assuming f_y is differentiable and the derivative of f_y ($h_y = \dot{f}_y$) is bounded, the state space form of (4-2) is

$$\begin{cases} \dot{\xi}_{y1} = \xi_{y2} \\ \dot{\xi}_{y2} = \xi_{y3} + b_y u_s \\ \dot{\xi}_{y3} = h_y \\ y = \xi_{y1} . \end{cases} \quad (5)$$

An ESO for (5) is designed as

$$\begin{aligned} \dot{\hat{\xi}}_{y1} &= \hat{\xi}_{y2} + l_{y1}(\xi_{y1} - \hat{\xi}_{y1}) \\ \dot{\hat{\xi}}_{y2} &= \hat{\xi}_{y2} + l_{y2}(\xi_{y2} - \hat{\xi}_{y2}) + b_y u_s \\ \hat{y} &= \hat{\xi}_{y1} \end{aligned} \quad (6)$$

where $L_y = \left[l_{y1}, l_{y2}, l_{y3}\right]^T$ is the observer gain. The observer gains are chosen such that the characteristic polynomial $s^3 + l_{y1}s^2 + l_{y2}s + l_{y3}$ is Hurwitz. For tuning simplicity, all the observer poles are placed at $-\omega_{oy}$. It results in the characteristic polynomial of (6) to be

$$\lambda_{oy}(s) = s^3 + l_{y1}s^2 + l_{y2}s + l_{y3} = \left(s + \omega_{oy}\right)^3 \quad (7)$$

where ω_{oy} is the observer bandwidth of the sense axis and $l_{y1} = 3\omega_{oy}, l_{y2} = 3\omega_{oy}^2, l_{y3} = \omega_{oy}^3$. This makes ω_{oy} the only tuning parameter for the observer. Thus the implementation process of the observer is much simplified.

Once the observer is designed and well tuned, its outputs will track $y, \dot{y}, f_y$ respectively. By canceling the effect of f_y using $\hat{\xi}_{y3}$, ADRC actively compensates for f_y in real time. The control law is designed as follows. First, the control law

$$u_s = \frac{u_0 - \hat{\xi}_{y3}}{b_y} \quad (8)$$

approximately reduces the original plant (4-2) to

$$\ddot{y} \approx u_0 \quad (9)$$

which is a much simple control problem to deal with. A simple controller can be designed as

$$u_0 = k_{y1}(r_y - \hat{\xi}_{y1}) + k_{y2}(\dot{r}_y - \hat{\xi}_{y2}) + \ddot{r}_y \quad (10)$$

where r_y is the desired trajectory of the sense axis. Note that a feedforward mechanism is employed in (10) for the purpose of reducing the tracking error. The controller gains are selected so that the closed-loop characteristic polynomial $s^2 + k_{y2}s + k_{y1}$ is Hurwitz. For tuning simplicity, all the controller poles are placed at $-\omega_{cy}$. Then the approximate closed-loop characteristic polynomial is

$$\lambda_{cy}(s) = s^2 + k_{y2}s + k_{y1} = \left(s + \omega_{cy}\right)^2 \quad (11)$$

where $k_{y1} = \omega_{cy}^2$, $k_{y2} = 2\omega_{cy}$. This makes ω_{cy}, the controller bandwidth, the only tuning parameter for the controller of the sense axis. This process is called bandwidth parameterization in [14], which greatly simplifies the control system design.

IV. ROTATION RATE ESTIMATION

Considering the sense axis of the MEMS gyroscope system, both Coriolis acceleration and Quadrature error terms are amplitude modulated signals centered at the resonant frequency of the drive axis. The only distinguishing characteristic between the two signals is that they have a relative phase shift of 90^0. Therefore we can take advantage of this characteristic to separate the undesired Quadrature errors from the useful Coriolis acceleration through the demodulation technique.

Applying the ESO (6) and the control law (8) and (10) to the MEMS gyroscope, we can drive the output of the drive axis x to the desired trajectory r_x with ideal amplitude and resonant frequency, force the output of sense axis y to zero, and accurately estimate the states of the drive and sense axes. Based on the accurate state estimation and the good tracking of the drive and sense axes, the rotation rate is estimated. The block diagram of ADRC for the sense axis control and rate estimation is shown in Fig. 4, where a demodulation block is used for the estimation of rotation rate. In Fig. 4, N_y represents the mechanical-thermal noise input to the sense axis and N_m represents the measurement noise (position noise) at the output of the sense axis [8].

The desired trajectory of the drive axis is $r_x = A\cos(\omega t)$. With the ideal tracking of ADRC, we have $x = r_x = A\cos(\omega t)$, and $\dot{x} = -A\omega\sin(\omega t)$. From (3), we have

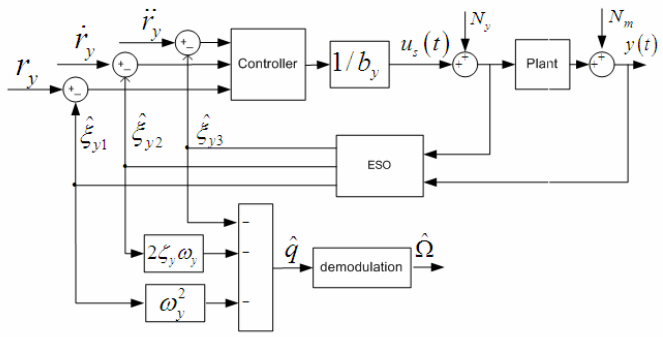

Fig. 4. Block diagram of the ADRC and rate estimation.

$$\omega_{xy}x + 2\Omega\dot{x} = -\left(f_y + 2\zeta_y\omega_y\dot{y} + \omega_y^2 y\right). \tag{12}$$

Let $q = \omega_{xy}x + 2\Omega\dot{x}$. It is assumed that the rotation rate is a sinusoidal signal [8], and $\Omega=\Omega_0\sin\left(2\pi f_{rate}t\right)$ where Ω_0 and f_{rate} are amplitude and frequency of the rotation rate. Then we have

$$\begin{aligned} q\cdot\sin(\omega t) &= \left(\omega_{xy}x + 2\Omega\dot{x}\right)\cdot\sin(\omega t) \\ &= \omega_{xy}A\cos(\omega t)\sin(\omega t) - 2\Omega A\omega\sin^2(\omega t) \\ &= \frac{1}{2}\omega_{xy}A\sin(2\omega t) - 2\Omega A\omega\frac{1-\cos(2\omega t)}{2} \\ &= \frac{1}{2}\omega_{xy}A\sin(2\omega t) + \Omega A\omega\cos(2\omega t) - \Omega A\omega \end{aligned} \tag{13}$$

where $\omega \gg 2\pi f_{rate}$ in the MEMS gyroscopes. In (13), the high frequency signals $\frac{1}{2}\omega_{xy}A\sin(2\omega t)$ and $\Omega A\omega\cos(2\omega t)$ will be filtered out through a low pass filter (LPF). Therefore the rotation rate Ω can be demodulated from the signal q by multiplying sin(ωt) and dividing by a gain introduced from modulation/demodulation, and filtering the resultant signal with a LPF, that is

$$\Omega = F_{LPF}\left(-\frac{q\cdot\sin(\omega t)}{A\omega}\right) \tag{14}$$

where $F_{LPF}(\cdot)$ represents the function of the LPF. With the information of the ESO, according to (12), the signal q in (14) can be estimated as follows

$$\hat{q} = -(\hat{f}_y + 2\zeta_y\omega_y\hat{\xi}_{y2} + \omega_y^2\hat{\xi}_{y1}). \tag{15}$$

The rotation rate can be estimated by

$$\hat{\Omega} = F_{LPF}\left(-\frac{\hat{q}\cdot\sin(\omega t)}{A\omega}\right). \tag{16}$$

The transfer function of the low-pass filter is chosen as

$$G_{LPF}(s) = \frac{1}{(\tau s+1)^2} \tag{17}$$

where τ is the time constant of the filter.

V. SIMULATION RESULTS

A control system based on ADRC is designed and simulated on a model of the Berkeley Z-axis gyroscope [21]. The key parameters are ω_n=81681.4 rad/sec, K=0.8338, ω_y=80864.6 rad/sec, ζ=4.5455×10^{-5}, ζ_y=3.125×10^{-4}, ω_{xy} = 6000 rad^2/sec^2, and m=2×10^{-9} kg. The design parameters $b_x = b_y = \frac{K}{m}$=4.169×10^8. The actual rotation rate is assumed to be a sinusoidal signal $\Omega=0.1\sin\left(2\pi f_{rate}t\right)$, and f_{rate}=50Hz. The reference signal for the drive axis is $r_x = A\cos(\omega t)$, where $\omega = 84194.7\text{rad/sec}$. Typically $A = 10^{-6}\,m$. We use $A = 50$ in "simulation units" to represent this [4]. The reference signal of the sense axis is $r_y = 0$. In the simulation, the mechanical-thermal noise is added to the drive axis, and the mechanical-thermal noise as well as the measurement noise is added to the sense axis. The PSD of mechanical-thermal noise for the drive axis is $2.4\times10^{-28}N^2\,\text{sec}$, and the one for the sense axis is $1.63\times10^{-27}N^2\,\text{sec}$. The PSD of measurement noise for the sense axis is $1.49\times10^{-27}N^2\,\text{sec}$ [8]. The controller and observer parameters for the drive axis are: $\omega_{cx} = 4.95\times10^5 rad/\text{sec}, \omega_{ox} = 2.45\times10^6 rad/\text{sec}$. The controller and observer parameters for the sense axis are: $\omega_{cy} = 5\times10^5 rad/\text{sec}, \omega_{oy} = 2\times10^7 rad/\text{sec}$. The time constant of LPF is $\tau = 6.7\times10^{-5}$ sec.

The output of the drive axis under the control of the ADRC is shown in Fig. 5. After approximate 1ms, the amplitude of the drive axis is maintained at 50 as desired, and the frequency of the drive axis is driven to the resonant frequency ω as expected. The output of the sense axis under the control of the ADRC is shown in Fig. 6. The stabilized output is around 0.01% of the uncontrolled amplitude of y, which shows that the sense axis is driven to almost zero. The rotation rate estimation at $f_{rate} = 50Hz$ is shown in Fig. 7. The estimated rotation rate can track the actual rotation rate after approximate 2.5ms and the steady-state peak error is about 1% of the actual rotation rate magnitude. This demonstrates that a fast and accurate estimation of the rotation rate is achieved.

To further investigate the robustness of ADRC against parameter variations, the system parameters are changed as follows: the natural frequency of the drive axis ω_n is increased by 10%, the natural frequency of the sense axis ω_y is increased by 20%, and the magnitude of the Quadrature error term is increased by 20%. With the plant parameter variations, the output of the drive axis, the output of the sense axis, and the rotation rate estimation are shown in Fig. 8, Fig. 9 and Fig. 10 respectively. Note that the tuning parameters of the ADRC and the rate frequency are not changed. The rotation rate estimations at $f_{rate} = 100Hz$ and $f_{rate} = 200Hz$ are shown in Fig. 11 and Fig. 12 respectively, without changing the parameters of the

ADRC and the LPF. With $f_{rate} = 100Hz$ and $f_{rate} = 200Hz$, the estimated rotation rates can track the actual rotation rate after approximate 2.5ms and the steady state peak errors are about 1% of the amplitude of actual rotation rate. The above simulation shows the strong robustness of the ADRC.

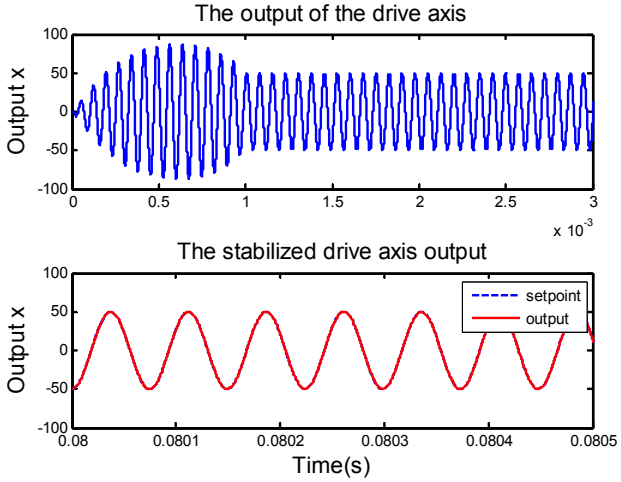

Fig. 5. The output of the drive axis.

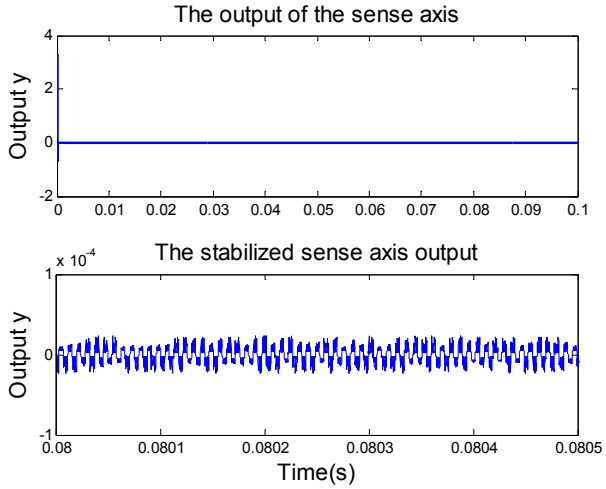

Fig. 6. The output of the sense axis.

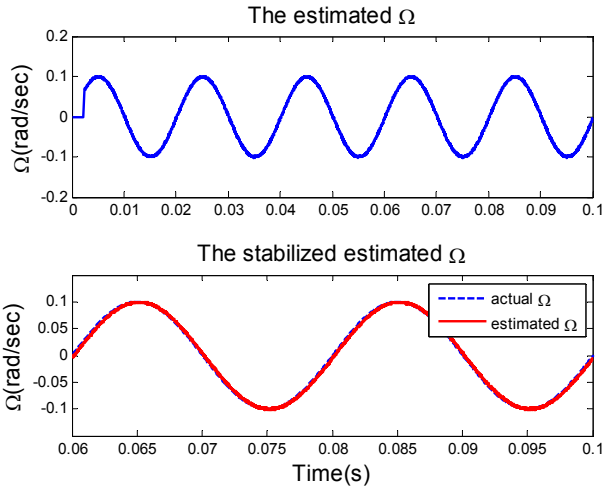

Fig. 7. The rotation rate estimation at $f_{rate} = 50Hz$.

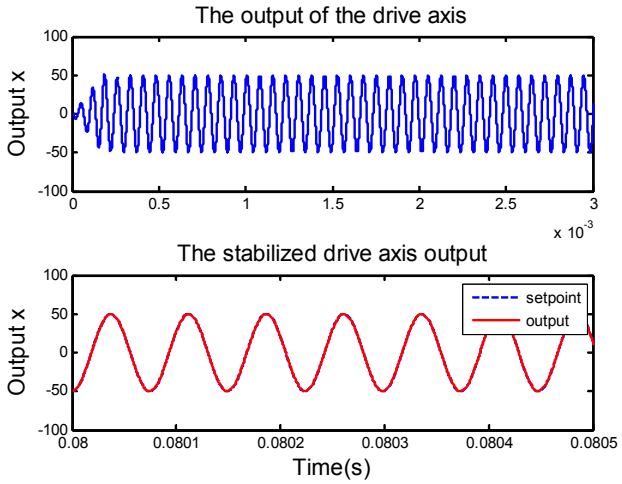

Fig. 8. The output of the drive axis with parameter variations.

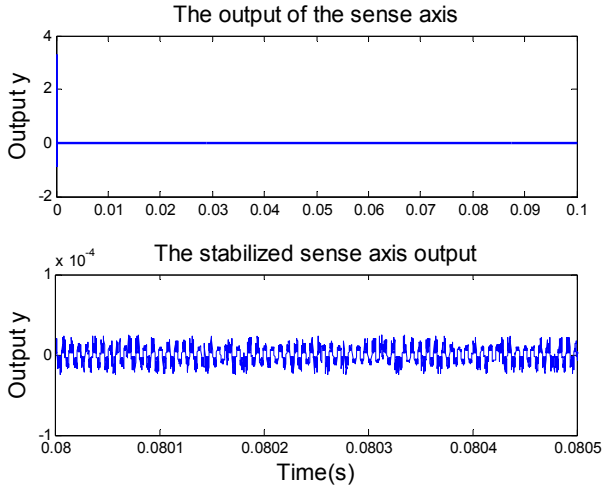

Fig. 9. The output of the sense axis with parameter variations.

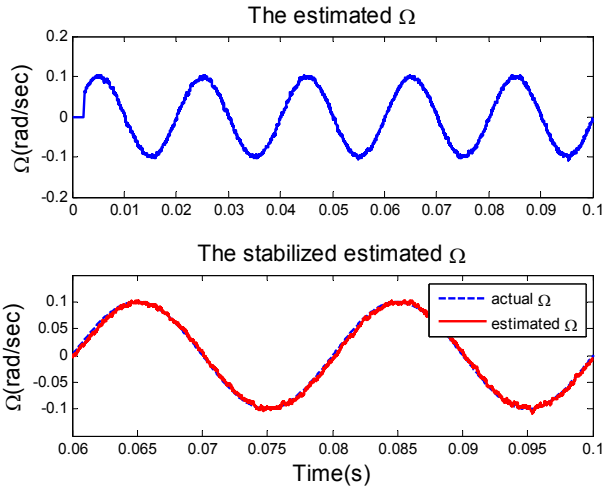

Fig. 10. The rotation rate estimation at $f_{rate} = 50Hz$ with parameter variations.

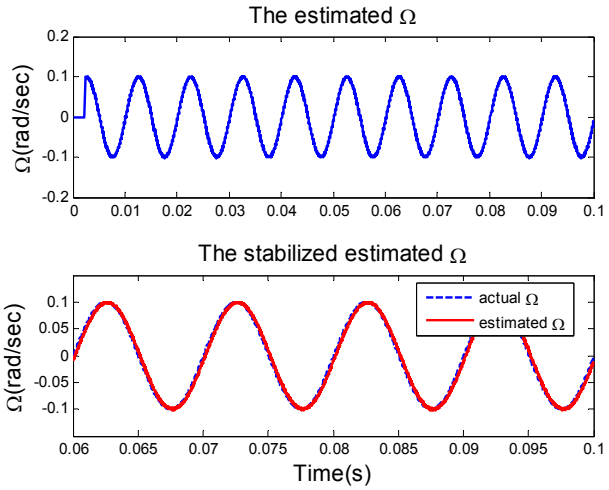

Fig. 11. The rotation rate estimation at $f_{rate} = 100Hz$.

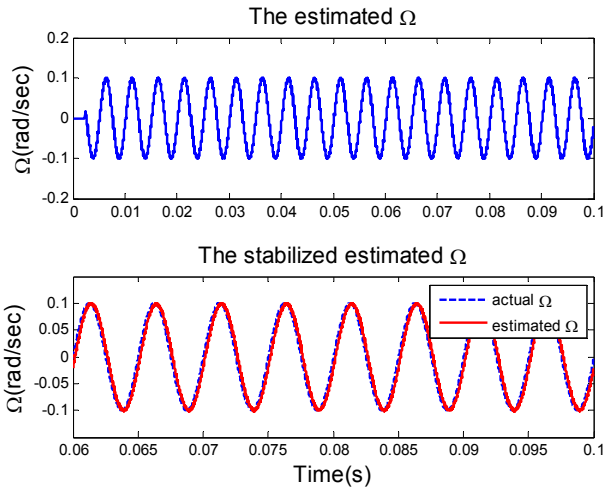

Fig. 12. The rotation rate estimation at $f_{rate} = 200Hz$.

VI. CONCLUSION

A novel control approach of active disturbance rejection is used to control the drive and sense axes of a vibrational MEMS gyroscope. Based on the accurate estimation of the internal plant dynamics and external disturbances of ESO, a demodulation technique is used to estimate the time-varying rotation rate. Since the ADRC does not require an accurate mathematical model of the plant, it is a good fit for the control and rate estimation of the MEMS gyroscope in the presence of noises and parameter variations. The simulation results demonstrated the high tracking performance and robustness of ADRC, as well as the fast and accurate estimation of the input rotation rate. Since most MEMS sensors have similar control problems to MEMS gyroscopes, i.e. precise amplitude and frequency control, disturbance rejection, and minimizing the effects of fabrication imperfection, ADRC provides a new solution. The range of ADRC applications will be greatly enlarged to include other MEMS sensors such as micro-accelerometers and pressure sensors in the future.

REFERENCES

[1] S. Park and R. Horowitz, "Adaptive Control for Z-axis MEMS Gyroscopes", *In Proceedings of American Control Conference*, pp.1223-1228, 2001.

[2] W. A. Clark, R. T. Howe, and R. Horowitz, "Surface micromachined Z-axis vibratory rate gyroscope," in *Tech. Dig. Solid-State Sensor and Actuator Workshop,* Hilton Head Island, SC, pp. 283–287, 1996.

[3] Y. Yazdi, F. Ayazi, and K. Najafi, "Micromachined inertial sensors," *in Proceedings of the IEEE*, vol. 86, no.8, pp.1640-1659, 1998.

[4] R. Leland, "Lyapunov based adaptive control of a MEMS gyroscope," *in proceedings of American Control Conference*, pp.3765-3770, 2002.

[5] R. P. Leland, Y. Lipkin, and A. Highsmith, "Adaptive oscillator control for a vibrational gyroscope," *in Proceedings of American Control Conference*, Denver, CO, pp. 3347-3352, June 2003.

[6] S. Park, "Adaptive control strategies for MEMS gyroscopes," PhD Dissertation, The University of California Berkely, 2000.

[7] A.M. Shkel, R. Horowitz, Ashwin A. Seshia, Sungsu Park, and Roger T. Howe, "Dynamics and control of micromachined gyroscopes," *in Proceedings of the American Control Conference*, pp. 2119-2124, 1999.

[8] S. Park and R. Horowitz, "Adaptive control for the conventional mode of operation of MEMS gyroscopes," *Journal of Microelectromechanical Systems*, vol. 12, no. 1, pp. 101-108, 2003.

[9] L. Dong and R.P. Leland, "The adaptive control system of a MEMS gyroscope with time-varying rotation rate," *in Proceedings of the American Control Conference*, pp. 3592-3597, 2005.

[10] L. Dong, "Adaptive control system for a vibrational MEMS gyroscope with time-varying rotation rates," PhD Dissertation, The University of Alabama, 2005.

[11] J. Han, "A class of extended state observers for uncertain systems,," *Control and Decision*, vol. 10, no. 1, pp. 85-88, 1995. (In Chinese)

[12] J. Han, "Nonlinear design methods for control systems," *Proc. of the 14th IFAC World Congress*, 1999.

[13] Z. Gao, Y. Huang, and J. Han, "An alternative paradigm for control system design," *In Proceedings of the IEEE conference on Decision and Control*, pp. 4578-4585, 2001.

[14] Z. Gao, "Scaling and parameterization based controller tuning," *In Proceedings of the American Control Conference*, pp. 4989-4996, 2003.

[15] Z. Gao, "Active disturbance rejection control: a paradigm shift in feedback control system design," *In Proceedings of the American Control Conference*, pp. 2399-2405, 2006.

[16] Z. Gao, S. Hu, and F. Jiang, "A novel motion control design approach based on active disturbance rejection," *in Proceedings of the IEEE Conference on Decision and Control*, pp. 4877-4882, 2001.

[17] Q. Zheng and Z. Gao, "Motion control opmitimization: problem and solutions," *Interntional Journal of Intelligent control and systems*, vol. 10, no. 4, pp. 269-276, 2006.

[18] Y. X. Su, B. Y. Duan, C. H. Zheng, Y . F. Zhang, G. D. Chen, and J. W. Mi, "Disturbance- rejection high-precision motion control of a Stewart Platform," *IEEE Transactions on Control System Technology*, vol. 12, no. 3, 2004.

[19] Y. Huang, K. Xu, and J. Han, "Flight control design using extended state observer and non-smooth feedback," *In Proceedings of the IEEE Conference on Decision and Control*, pp. 223-228, 2001.

[20] B. Sun and Z. Gao, "A DSP-based active disturbance rejection control design for a 1KW H-bridge DC-DC power converter," *IEEE Trans. on Industrial Electronics*, vol. 52, no. 5, pp. 1271-1277, 2005.

[21] W. A. Clark, "Micromachined vibratory rate gyroscope," PhD Dissertation, The University of California Berkely, 1997.